



Functional guanine–arginine interaction between tRNA^{Pro} and prolyl-tRNA synthetase that couples binding and catalysis

Brian Burke^{a,1}, Songon An^{a,2}, Karin Musier-Forsyth^{b,c,*}

^a Department of Chemistry, University of Minnesota, 207 Pleasant Street Southeast, Minneapolis, MN 55455, USA

^b Department of Chemistry, The Ohio State University, 100 West 18th Avenue, Columbus, OH 43210, USA

^c Department of Biochemistry, The Ohio State University, Columbus, OH 43210, USA

ARTICLE INFO

Article history:

Received 9 November 2007

Received in revised form 26 April 2008

Accepted 29 April 2008

Available online 10 May 2008

Keywords:

Aminoacyl-tRNA synthetases

Prolyl-tRNA synthetase

Oxidative cross-linking

8-oxo-guanosine

RNA–protein interactions

Coupling network

ABSTRACT

Aminoacyl-tRNA synthetases catalyze the attachment of specific amino acids to their cognate tRNAs. Specific aminoacylation is dictated by a set of recognition elements that mark tRNA molecules as substrates for particular synthetases. *Escherichia coli* prolyl-tRNA synthetase (ProRS) has previously been shown to recognize specific bases of tRNA^{Pro} in both the anticodon domain, which mediate initial complex formation, and in the acceptor stem, which is proximal to the site of catalysis. In this work, we unambiguously define the molecular interaction between *E. coli* ProRS and the acceptor stem of cognate tRNA^{Pro}. Oxidative cross-linking studies using 2'-deoxy-8-oxo-7,8-dihydroguanosine-containing proline tRNAs identify a direct interaction between a critical arginine residue (R144) in the active site of *E. coli* ProRS and the G72 residue in the acceptor stem of tRNA^{Pro}. Assays conducted with motif 2 loop variants and tRNA mutants wherein specific atomic groups of G72 were deleted, are consistent with a functionally important hydrogen-bonding network between R144 and the major groove of G72. These results taken together with previous studies suggest that breaking this key contact uncouples the allosteric interaction between the anticodon domain and the aminoacylation active site, providing new insights into the communication network that governs the synthetase–tRNA interaction.

© 2008 Elsevier B.V. All rights reserved.

1. Introduction

Aminoacyl-tRNA synthetases catalyze the attachment of specific amino acids to their cognate tRNAs. This reaction is critical for ensuring high fidelity translation of the genetic code. Specific tRNA binding and aminoacylation are dictated by a set of recognition elements primarily found in the anticodon and acceptor stem of the tRNA [1]. Despite the availability of a large number of X-ray crystal structures of synthetase–tRNA complexes, in most systems, the path of communication between the anticodon recognition event and the site of catalysis, which is located ~70 Å away, is unknown and remains a major open question in the field. Both short- and long-range thermal motions and an allosteric network of functional protein–RNA interactions are likely to play an important role in this process [2–6].

Escherichia coli prolyl-tRNA synthetase (ProRS) is a class II synthetase previously shown to recognize elements in both the anticodon and acceptor stem of tRNA^{Pro} [7,8]. These data are in good agreement

with the X-ray crystal structure of *Thermus thermophilus* ProRS complexed to the anticodon of its cognate tRNA [9]. Although a co-crystal structure of a ProRS with the tRNA acceptor stem bound has not been reported to date, biochemical data have shown that *E. coli* ProRS recognizes major groove elements of acceptor stem nucleotides A73 and G72 of *E. coli* tRNA^{Pro} [10]. The latter position is unique to tRNA^{Pro} isoacceptors in *E. coli* [7,11]. Furthermore, residue R144 of *E. coli* ProRS, which is located in the so-called “motif 2 loop” sequence, ¹⁴³VRPRF¹⁴⁷, is critical for efficient aminoacylation. An R144C substitution completely abolishes tRNA charging, but has no effect on amino acid activation [10]. Cross-linking experiments confirmed the close proximity between the motif 2 loop and the tRNA acceptor stem [10]. Based on these data, a specific interaction between the motif 2 loop and the acceptor stem was proposed [10]. However, due to the length and location of the tether used in the previous cross-linking studies, the exact nature of the interaction could not be elucidated.

A novel method of oxidatively inducing DNA–protein cross-links has been reported using 2'-deoxy-8-oxo-7,8-dihydroguanosine (OG)-substituted DNA [12,13]. In the presence of Na₂IrCl₆, OG is readily oxidized to create an electron-deficient center highly susceptible to attack by a nearby nucleophilic protein side chain [12,14]. Since cross-link formation requires that two functional groups be within hydrogen-bonding distance, interactions can be mapped with high precision using this approach. Furthermore, studies are consistent

* Corresponding author. Tel.: +1 614 292 2021; fax: +1 614 688 5402.

E-mail address: musier@chemistry.ohio-state.edu (K. Musier-Forsyth).

¹ Current address: Novartis Vaccines and Diagnostics, 4560 Horton Street, Emeryville, CA 94608, USA.

² Current address: Department of Chemistry, The Pennsylvania State University, 104 Chemistry Building, University Park, PA 16802, USA.

Table 1
Effect of single amino acid changes at position 144 in the motif 2 loop of *E. coli* ProRS on aminoacylation of *E. coli* tRNA^{Pro} transcripts^a

ProRS mutation	k_{cat} (s ⁻¹)	K_M (μM)	k_{cat}/K_M (s ⁻¹ μM ⁻¹)	k_{cat}/K_M (relative)	x-fold change
Wild-type	0.35	18.0	1.8×10^{-2}	1.0	1.0
R144K	2.5×10^{-4}	11.0	3.7×10^{-5}	2.1×10^{-3}	–480
R144L	1.0×10^{-4}	10.3	2.1×10^{-5}	1.1×10^{-3}	–870

^a Assays were performed at least twice with a difference of <2-fold between trials.

with a mechanism of cross-linking involving nucleophilic attack of an amino acid side chain (e.g., lysine or arginine) at C5 in the major groove of oxidized OG. Although to our knowledge this method has never been applied to the study of RNA–protein interactions, this appeared to be a promising approach in our system for fine structure mapping of the ProRS motif 2 loop–tRNA^{Pro} acceptor stem interaction.

In this work, the molecular interactions between *E. coli* ProRS and the acceptor stem of cognate tRNA^{Pro} are elucidated using aminoacylation assays and cross-linking with OG-containing tRNAs. The results presented here strongly support a direct hydrogen-bonding interaction between a critical arginine residue in the active site of *E. coli* ProRS and major groove functional groups of G72 in the acceptor stem of tRNA^{Pro}. We hypothesize that the R144–G72 interaction constitutes a key component of the network that communicates the anticodon recognition event to the site of catalysis. Thus, more precisely defining this hydrogen-bonding network contributes to our understanding of allosteric coupling junctions influencing long-distance communication in this system.

2. Materials and methods

2.1. Enzyme purification and site-directed mutagenesis of ProRS

Purification of His-tagged wild-type *E. coli* ProRS was accomplished as described previously [15]. Site-directed mutagenesis of the motif 2 loop residues was accomplished by overlap extension PCR [16] using DNA primers encoding the desired changes. There is only one cysteine in wild-type *E. coli* ProRS and this change was previously shown to result in only a minor reduction in aminoacylation efficiency [10]. Due to their availability, three motif 2 mutant proteins (V143C, R144C, and R146C) additionally containing a C443G mutation were also studied in this work. The entire gene was sequenced to verify the specified mutation and to ensure that the mutagenesis procedure did not introduce undesired mutations. *E. coli* strain SG13009 [pREP4] (Qiagen) was transformed with the mutant plasmids for overexpression and purification, which were performed as described for the wild-type enzyme. ProRS concentrations were based on active-site titrations determined by the adenylate burst assay [17].

2.2. RNA preparation

Semi-synthetic *E. coli* ΔC1-tRNA^{Pro} was prepared from two fragments as previously described [18]. The omission of C1 facilitates in vitro transcription and results in a tRNA substrate that is ~3-fold more active than a C1-containing tRNA^{Pro} transcript. 5'-3/4-length (nucleotides 1–57) fragment of tRNA^{Pro} was in vitro transcribed using a DNA template linearized by BstBI digestion of the plasmid used to obtain full-length *E. coli* ΔC1-tRNA^{Pro} as described [8]. The 3'-16-mer fragment was chemically synthesized using the phosphoramidite method on an Expedite™ 8909 Nucleic Acid Synthesis System (PerSeptive Biosystems). The modified deoxynucleotides 8-oxo-7,8-dihydro-guanosine (OG), 2-aminopurine (2AP), 7-deaza-A (7A), and 7-deaza-G (7G) (all from Glen Research), were incorporated into position 72 or 73 (tRNA numbering) of the synthetic 3'-16-mer during automated chemical synthesis. Synthetic oligonucleotides were purified on 16% denaturing polyacrylamide gels followed by elution and work-up as described [18]. [³²P]-labeling of the 5'-end of the 16-mer oligonucleotides was carried out following the manufacturer's protocol using [γ-³²P]-ATP (New England Nuclear) and polynucleotide kinase (New England Biolabs). Semi-synthetic tRNA molecules were generated by annealing 1:1 ratios of 5'-3/4-length tRNAs to 3'-16-mer RNA fragments at 60 °C for 3 min, followed by addition of MgCl₂ to 10 mM final concentration, cooling at room temperature for 5 min and placement on ice.

2.3. Aminoacylation assays

Aminoacylation assays were carried out essentially as described previously [15,19]. Kinetic assays using wild-type, R144K and R144L *E. coli* ProRS were performed with 50–200 nM enzyme and 2–20 μM *E. coli* ΔC1-tRNA^{Pro}. The kinetic constants were derived from Lineweaver–Burk plots. In the case of semi-synthetic tRNAs containing acceptor

stem mutations at position 72 or 73, relative k_{cat}/K_M values were determined either from Lineweaver–Burk plots or from the initial rates of aminoacylation, which are proportional to RNA concentration under the conditions used for these experiments. Thus, $V_0/[S]$ is an accurate reflection of k_{cat}/K_M .

2.4. Cross-linking reactions

RNA–protein cross-linking reactions were carried out using a modification of the procedure described by Burrows et al. [12]. Wild-type or mutant ProRS (1–5 μM) and wild-type or OG72-containing semi-synthetic 5'-[³²P]-ΔC1-tRNA^{Pro} (5–10 μM) were incubated in 50 mM HEPES (pH 7.5) for 5 min at room temperature, followed by addition of 100 μM Na₂IrCl₆ (Alfa Aesar). In some experiments, proline, ATP, proline+ATP, or 5'-O-[N-(L-prolyl)sulfamoyl]adenosine (Pro-AMS) were added to a final concentration of 20 μM prior to addition of Na₂IrCl₆. After 4 h of incubation at room temperature, reactions were quenched with 50 mM EDTA (pH 8.0). Reaction mixtures were loaded onto 8% sodium dodecyl sulfate-polyacrylamide gels, visualized, and quantified via phosphorimaging analysis of the dried gel.

3. Results and discussion

We first incorporated amino acid substitutions lysine and leucine at position 144 in the motif 2 loop of *E. coli* ProRS. Mutation of the positively charged R144 side chain to a neutral leucine residue resulted in an 870-fold reduced aminoacylation catalytic efficiency (Table 1). Even the conservative change to lysine resulted in a large 480-fold decrease in k_{cat}/K_M (Table 1). Interestingly, in both cases, the defect was entirely in the k_{cat} parameter, with little effect on the K_M . These data confirmed the sensitivity of ProRS to changes at this site and showed that the defect was not at the binding step.

Previously, we hypothesized that residues in the motif 2 loop interact closely with acceptor stem residues G72 and A73. If a hydrogen-bonding interaction between R144 and G72 and/or A73 occurs, the decrease in aminoacylation caused by mutations at these nucleotides [8] may be completely or partially suppressed by the R144 mutants. We indeed demonstrate in this work that aminoacylation of G72A-tRNA^{Pro} is reduced 170-fold compared to wild-type tRNA^{Pro} when assayed with wild-type ProRS, whereas only a 2.6-fold decrease is observed with R144K ProRS (relative to charging of wild-type tRNA^{Pro} by R144K ProRS) (Table 2). Interestingly, R144L ProRS actually prefers G72A-tRNA^{Pro} as a substrate; the aminoacylation efficiency measured with this variant is 2.4-fold greater relative to aminoacylation of wild-type tRNA^{Pro} (Table 2). These results are consistent with a functional interaction between position 144 of ProRS and G72 of tRNA^{Pro}. However, similar results were obtained with an A73G tRNA variant (Table 2). Whereas the k_{cat}/K_M of this tRNA is 175-fold reduced in the presence of wild-type ProRS, R144K and R144L ProRS variants are not sensitive to the change of A73 to G.

We also reported that mutations of other positions in the motif 2 loop have significant but much more modest (3- to 80-fold) effects on aminoacylation [10]. To confirm the positional specificity of the G72/A73 interaction within the motif 2 loop, we further tested two

Table 2
Ratio of k_{cat}/K_M for aminoacylation of wild-type and mutant tRNA^{Pro} by wild-type and mutant ProRS^a

	G72A	A73G	2AP72	7G72	7A73
ProRS (WT)	170	175	30	52	23
R144K (–480)	2.6	1.0	2.5	2.1	7.4
R144L (–870)	0.42	0.91	0.43	0.06	18
V143C (–3)	230	310	ND	ND	ND
R146C (–79)	>10 ⁶	>10 ⁶	ND	ND	ND

^a 2AP is 2'-deoxy-2-aminopurine, 7G is 2'-deoxy-7-deaza-G, and 7A is 2'-deoxy-7-deaza-A. The 2'-hydroxyl group was previously shown to be dispensable at positions 72 [12] and 73 [5]. The ratios were obtained as follows: $(k_{cat}/K_M)_{wild\text{-type tRNA}} / (k_{cat}/K_M)_{mutant\text{ tRNA}}$. ND stands for not determined. The numbers in parenthesis (left column) indicate the fold decrease in the wild-type (WT) tRNA^{Pro} aminoacylation efficiency of the indicated mutant ProRS, relative to WT ProRS (in the case of R144K and R144L) or relative to C443G ProRS (in the case of V143C and R146C, see Materials and methods). All assays were performed at least twice with a difference of <2-fold between trials.

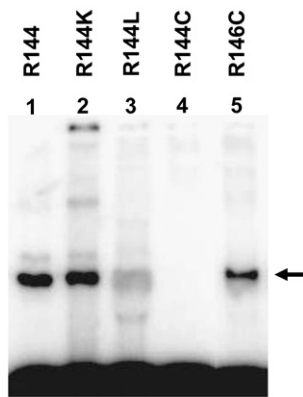


Fig. 1. Denaturing polyacrylamide gel (8%) showing the results of oxidative cross-linking of semi-synthetic OG72-tRNA^{Pro} to wild-type (lane 1) and mutated *E. coli* ProRS (lane 2–5). As discussed in the Materials and methods, R144C (lane 4) and R146C (lane 5) ProRS variants contain an additional C443G mutation. The cross-linked adduct is indicated by an arrow.

additional motif 2 loop mutants (V143C and R146C) that were previously reported to result in 3-fold and 79-fold decreases in k_{cat}/K_M , respectively. Here we report that, in contrast to the results obtained with R144 variants, V143C ProRS and R146C ProRS displayed large decreases (230-fold and $>10^6$ -fold, respectively) in aminoacylation of G72A-tRNA^{Pro} relative to charging of wild-type tRNA^{Pro} (Table 2). Similar results were obtained with A73G-tRNA^{Pro}. These results show that activity changes due to V143C and R146C mutations are not suppressed by mutation of G72A and A73G of tRNA^{Pro}, and therefore, they do not support a functional interaction between V143 or R146 and positions 72/73 of the acceptor stem.

Nucleotide base changes such as those described above may also result in indirect effects due to conformational or stacking differences induced by the mutations. More subtle atomic group substitutions or deletions are less likely to have these indirect effects. To further define the nature of the interaction between R144 and G72/A73, atomic group mutants were incorporated into semi-synthetic tRNA^{Pro} constructs. Substitution of 2-aminopurine at position 72, which removes the major groove 6-keto oxygen, results in a 30-fold decrease in aminoacylation by wild-type ProRS, but only a 2.5-fold decrease with R144K ProRS (Table 2). Similar to the G72A variant, this mutant displays slightly increased activity with R144L. These data support a direct hydrogen-bonding interaction between R144 and the major groove oxygen of G72. Substitution of the N7 position with a carbon by incorporation of 7-deaza-G72, results in a 52-fold decrease in charging by wild-type ProRS but only a 2.1-fold decrease in the case of R144K ProRS and a striking 17-fold increase with R144L. The latter may be due to more favorable nonpolar packing between the leucine side chain and the carbon at position 7 (in contrast to the unfavorable polar surface area of N7) [20]. In contrast to the results obtained at position 72, the effects of substituting neighboring base A73 with 7-deaza-A are not significantly suppressed (3-fold or less) by changes at R144 (Table 2). In particular, the R144L variant is as sensitive to the 7-deaza-A73 change as wild-type ProRS. Taken together, we conclude that R144 interacts preferentially with G72 through two hydrogen-bonding interactions with the 6-keto oxygen and N7 position in the major groove.

We next incorporated OG into the acceptor stem of semi-synthetic *E. coli* tRNA^{Pro} at the critical G72 position. This substitution resulted in only a small (<2 -fold) decrease in aminoacylation by wild-type ProRS (data not shown). Previous work also showed that deoxynucleotide substitution at G72 resulted in a minor (1.2-fold) reduction in k_{cat}/K_M [18]. Unmodified and OG-containing tRNAs were incubated with wild-type, R144K, R144L, or R144C *E. coli* ProRS and Na₂IrCl₆. As mentioned earlier, these mutations on ProRS did not negatively affect the K_M values for tRNA^{Pro} (Table 1), suggesting that the defects are not in the

binding step. Following the cross-linking reactions, samples were analyzed on denaturing polyacrylamide gels (Fig. 1).

As shown in Fig. 1, a cross-linked adduct is detected when wild-type and R144K ProRS are incubated with OG72-tRNA under oxidative conditions (lanes 1 and 2). Cross-linking is dependent upon the presence of an arginine or lysine residue at position 144, as R144L ProRS shows only slight non-specific (see below) cross-linking (lane 3) and no cross-link is detected with R144C ProRS (lane 4). Cross-linking is not observed in the control reactions using unmodified tRNA^{Pro} (data not shown). These results support the conclusion that residue 144 is in close proximity (~ 1.5 Å) to G72 and that both arginine and lysine side chains can react with oxidized OG, as previously reported [13,14]. The lack of cross-link formation with R144C and R144L ProRS suggests that the nearby motif 2 loop residue, R146, is not involved in close interaction with G72 and cannot substitute for the function of R144. This result is consistent with the kinetic data for R146C ProRS, which also suggested that R146 is not functionally involved in interaction with G72/A73 (Table 2). To confirm this hypothesis further, we showed that a R146C ProRS variant cross-links to OG72-tRNA, albeit with an ~ 1.3 -fold reduced yield relative to wild-type or R144K ProRS (Fig. 1, lane 5), which may be due to non-optimal positioning of the R144 side chain with respect to the major groove of OG72. Taken together, these data support the role of R144 in specific cross-link formation to OG72.

The crystal structure of *T. thermophilus* ProRS bound to prolyl-adenylate shows a close interaction between the adenylate and the motif 2 loop, as well as an ordering and movement of the loop upon substrate binding [21]. To gain further support for the specific involvement of *E. coli* ProRS motif 2 loop residues in cross-link formation, we performed cross-linking studies in the presence of proline, ATP, proline and ATP, or a non-hydrolysable sulfamoyl analogue of prolyl-adenylate, Pro-AMS.

The efficiency of OG72-tRNA^{Pro} cross-linking to R144K ProRS is suppressed only slightly in the presence of proline alone (~ 1.4 -fold) or ATP alone (~ 2.8 -fold), but is more significantly reduced in the presence of Pro-AMS (~ 4.5 -fold) or both proline and ATP (~ 5.9 -fold) (Fig. 2). These results support the proximity of the observed cross-linked adduct to the aminoacylation active site, and suggest either that conformational changes upon adenylate formation result in the reduced level of cross-link formation, or that the adenylate sterically blocks interaction of G72 with active-site residues. In contrast, the slight cross-linking observed with R144L ProRS (Fig. 1, lane 3) is not affected by the presence of substrates (data not shown), indicating that the cross-linking observed with this variant is likely due to non-specific interactions outside the active site.

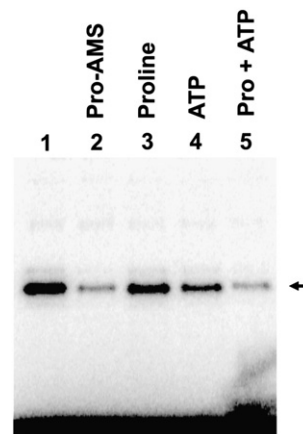


Fig. 2. Denaturing polyacrylamide gel (8%) showing the results of oxidative cross-linking of semi-synthetic OG72-tRNA^{Pro} to R144K *E. coli* ProRS in the absence (lane 1) and presence of the indicated substrates (lanes 3–5) or the Pro-AMS adenylate analogue (lane 2). The cross-linked adduct is indicated by an arrow.

In summary, mutagenesis and kinetic data, together with a novel cross-linking approach were used to identify a specific hydrogen-bonding interaction between the arginine side chain at position 144 of the motif 2 loop of *E. coli* ProRS and the major groove functional groups of G72 in the tRNA^{Pro} acceptor stem. Changes at R144 do not substantially alter the Michaelis constant for tRNA, but significantly affect the k_{cat} parameter. Transfer RNA aminoacylation has been described as a multistep process involving initial formation of an “encounter complex”, which generally depends on specific anticodon interactions, followed by an “accommodation” process that involves conformational changes in both partners resulting in correct positioning of the CCA end in the active site [22]. We propose that the R144–G72 contact plays a critical role in the latter process, in effect coupling the anticodon recognition/binding event to catalysis by optimally positioning the CCA-3' end into the active site. The results also indicate that A73 is likely to be involved in a hydrogen-bonding network involving nearby motif 2 loop residues, although the exact nature of this interaction is not yet clear.

Based on deposited structures in the Protein Data Bank (<http://www.pdb.org>), arginine–guanine interactions are the most abundant contacts found in the amino acid–nucleotide interaction database (AANT; <http://aant.icmb.utexas.edu/>) [23]. Thus, the biochemical approaches described here should be widely applicable to the identification of nucleic acid–protein interactions for which high resolution structural information obtained by NMR or X-ray crystallography is not available.

Acknowledgements

We thank Drs. Penny J. Beuning and Abbey E. Rosen for synthesizing the synthetic oligonucleotides used in this study. We would also like to thank Ms. Carmen Silvers for assistance with purification of ProRS mutants. This work was funded by National Institutes of Health grant GM49928 (K.M.-F.) and T32 GM08277 (B.B.).

References

- [1] R. Giegé, M. Sissler, C. Florentz, Universal rules and idiosyncratic features in tRNA identity, *Nucleic Acids Res.* 26 (1998) 5017–5035.
- [2] A. Ghosh, S. Vishveshwara, A study of communication pathways in methionyl-tRNA synthetase by molecular dynamics simulations and structure network analysis, *Proc. Natl. Acad. Sci. U. S. A.* 104 (2007) 15711–15716.
- [3] S. Hammes-Schiffer, S.J. Benkovic, Relating protein motion to catalysis, *Annu. Rev. Biochem.* 75 (2006) 519–541.
- [4] M.E. Budiman, M.H. Knaggs, J.S. Fetrow, R.W. Alexander, Using molecular dynamics to map interaction networks in an aminoacyl-tRNA synthetase, *Proteins* 68 (2007) 670–689.
- [5] J.J. Perona, Y.M. Hou, Indirect readout of tRNA for aminoacylation, *Biochemistry* 46 (2007) 10419–10432.
- [6] E.A. First, A.R. Fersht, Analysis of the role of the KMSKS loop in the catalytic mechanism of the tyrosyl-tRNA synthetase using multimutant cycles, *Biochemistry* 34 (1995) 5030–5043.
- [7] W.H. McClain, J. Schneider, K. Gabriel, Distinctive acceptor-end structure and other determinants of *Escherichia coli* tRNA(Pro) identity, *Nucleic Acids Res.* 22 (1994) 522–529.
- [8] H. Liu, R. Peterson, J. Kessler, K. Musier-Forsyth, Molecular recognition of tRNA(Pro) by *Escherichia coli* proline tRNA synthetase in vitro, *Nucleic Acids Res.* 23 (1995) 165–169.
- [9] A. Yaremchuk, S. Cusack, M. Tukalo, Crystal structure of a eukaryote/archaeon-like prolyl-tRNA synthetase and its complex with tRNAPro(CGG), *EMBO J.* 19 (2000) 4745–4758.
- [10] B. Burke, F. Yang, F. Chen, C. Stehlin, B. Chan, K. Musier-Forsyth, Evolutionary coadaptation of the motif 2–acceptor stem interaction in the class II prolyl-tRNA synthetase system, *Biochemistry* 39 (2000) 15540–15547.
- [11] M. Sprinzl, K.S. Vassilenko, Compilation of tRNA sequences and sequences of tRNA genes, *Nucleic Acids Res.* 33 (2005) D139–D140.
- [12] R.P. Hickerson, C.L. Chepanoske, S.D. Williams, S.S. David, C.J. Burrows, Mechanism-based DNA–protein cross-linking of MutY via oxidation of 8-oxoguanosine, *J. Am. Chem. Soc.* 121 (1999) 9901–9902.
- [13] M.E. Johansen, J.G. Muller, X. Xu, C.J. Burrows, Oxidatively induced DNA–protein cross-linking between single-stranded binding protein and oligodeoxynucleotides containing 8-oxo-7,8-dihydro-2'-deoxyguanosine, *Biochemistry* 44 (2005) 5660–5671.
- [14] J.G. Muller, V. Duarte, R.P. Hickerson, C.J. Burrows, Gel electrophoretic detection of 7,8-dihydro-8-oxoguanine and 7,8-dihydro-8-oxoadenine via oxidation by Ir (IV), *Nucleic Acids Res.* 26 (1998) 2247–2249.
- [15] D. Heacock, C.J. Forsyth, K. Shiba, K. Musier-Forsyth, Synthesis and aminoacyl-tRNA synthetase inhibitory activity of prolyl adenylate analogs, *Bioorganic Chemistry* 24 (1996) 273–289.
- [16] R.M. Horton, L.R. Pease, Directed mutagenesis, in: M.J. McPherson (Ed.), IRL press, New York, 1991, pp. 217–247.
- [17] A.R. Fersht, J.S. Ashford, C.J. Bruton, R. Jakes, G.L. Koch, B.S. Hartley, Active site titration and aminoacyl adenylate binding stoichiometry of aminoacyl-tRNA synthetases, *Biochemistry* 14 (1975) 1–4.
- [18] L.P. Yap, K. Musier-Forsyth, Transfer RNA aminoacylation: identification of a critical ribose 2'-hydroxyl-base interaction, *RNA* 1 (1995) 418–424.
- [19] C. Stehlin, D.H. Heacock, H. Liu, K. Musier-Forsyth, Chemical modification and site-directed mutagenesis of the single cysteine in motif 3 of class II *Escherichia coli* prolyl-tRNA synthetase, *Biochemistry* 36 (1997) 2932–2938.
- [20] J. Ashworth, J.J. Havranek, C.M. Duarte, D. Sussman, R.J. Monnat Jr., B.L. Stoddard, D. Baker, Computational redesign of endonuclease DNA binding and cleavage specificity, *Nature* 441 (2006) 656–659.
- [21] A. Yaremchuk, M. Tukalo, M. Grotli, S. Cusack, A succession of substrate induced conformational changes ensures the amino acid specificity of *Thermus thermophilus* prolyl-tRNA synthetase: comparison with histidyl-tRNA synthetase, *J. Mol. Biol.* 309 (2001) 989–1002.
- [22] E.C. Guth, C.S. Francklyn, Kinetic discrimination of tRNA identity by the conserved motif 2 loop of a class II aminoacyl-tRNA synthetase, *Mol. Cell* 25 (2007) 531–542.
- [23] M.M. Hoffman, M.A. Khrapov, J.C. Cox, J. Yao, L. Tong, A.D. Ellington, AANT: the Amino Acid–Nucleotide Interaction Database, *Nucleic Acids Res.* 32 (2004) D174–181.